Isı Bilimi ve Tekniği Dergisi, 38, 1, 55-64, 2018
J. of Thermal Science and Technology

ISSN 1300-3615

NUMERICAL INVESTIGATION OF THE FLAME LOCATION OF TURBULENT PREMIXED COMBUSTION IN A DIFFUSER BURNER EXPOSED TO VARIOUS TURBULENCE INTENSITIES AND TURBULENCE LENGTH SCALES

Ibrahim Thamer NAZZAL*, and Özgür ERTUNÇ***
* Mechanical Engineering Department, Özyeğin University, Çekmeköy, Istanbul 34794, Turkey
thamer.nazzal@ozu.edu.tr, ozgur.ertunc@ozyegin.edu.tr
** Mechanical Engineering Department, College of Engineering, Tikrit University, Tikrit, Iraq

(Geliş Tarihi: 20.03.2017, Kabul Tarihi: 15.12.2017)

Abstract: This study aims to investigate the response of the flame location of a turbulent premixed flame that has been exposed to various turbulence intensities and turbulence length scales. A diffuser-type burner is used to reveal the influence of turbulence intensity and turbulence length scales on the flame location of premixed propane–air flames without changing the inlet velocity of the fuel. Numerical simulations are performed for the turbulent premixed propane flames by using a coherent flame model under steady-state conditions. Results show that the flame location moves toward the inlet of the diffuser combustor with an increase in turbulence intensity for moderate and high turbulence length scales. The behavior of the flame location is different for the low turbulence length scale. The flame location initially decreases with an increase in turbulence intensity and subsequently stabilizes. Furthermore, the maximum flame area density is shown to increase with an increase in the turbulence intensity and the turbulence length scale, as the flame moves toward the inlet in these cases. It is clearly documented how turbulence intensity and turbulence length scale simultaneously influence the flame area density, flame shape, and flame location in a diffuser-type burner.
Keywords: Premixed turbulent combustion, flame area density, turbulence intensity, turbulence length scale, coherent flame model.

DİFÜZÖR TİPİ YANMA ODASINDA GERÇEKLEŞEN ÖN KARIŞIMLI TÜRBÜLANSLI YANMADA ORTAYA ÇIKAN ALEVİN KONUMUNUN TÜRBÜLANS YOĞUNLUĞU VE TÜRBÜLANS UZUNLUK ÖLÇÜSÜ İLE DEĞİŞİMİNİN SAYISAL OLARAK İNCELENMESİ

Özet: Bu makalenin amacı, ön karışımlı yanma sonucu oluşan alevin, çeşitli türbülans yoğunluklarına ve türbülans uzunluk ölçeğine maruz kalması sonucu oluşan alev yeri değişikliğini incelemektir. Yakıtın yanma odasına giriş hızını değiştirmeden, sadece türbülans yoğunluğunun ve türbülans uzunluk ölçeğinin alev yeri üstüne etkisini görebilmek için araştırmalar difüzör tipi yanma odasında gerçekleştirilmiştir. Propanın türbülanslı ön karışımlı yanma simulasyonları tutarlı alev modeli (coherent flame model) kullanılarak kararlı akış rejiminde gerçekleştirilmiştir. Orta ve yüksek türbülans uzunluk ölçeği kullanıldığında türbülans yoğunluğundaki artış ile alevin difüzörün girişine doğru hareket ettiği gözlemlenmiştir. Düşük uzunluk ölçeği kullanılarak gerçekleştirilen simulasyonlarda, alev türbülans yoğunluğunun artması ile girişe doğru yaklaştığı ancak türbülans yoğunluğunun daha da arttılmasına rağmen alev konumunda kayda değer bir değişiklik olmadığı gözlemlenmiştir. Sonuçlar, türbülans yoğunluğu ve türbülans uzunluk ölçeğindeki artışın, maksimum alev alan yoğunluğunu arttırdığını göstermektedir. Dahası türbülans yoğunluğunun ve uzunluk ölçeğinin alev alan yoğunluğu, alevin şekli ve konumu üzerinde aynı anda etkili olduğu gösterilmiştir.
Anahtar Kelimler : Türbülanslı ön karışımlı yanma, alev alan yoğunluğu, türbülans yoğunluğu, türbülans uzunluk ölçeği, tutarlı alev modeli.

NOMENCLATURE

A	Area [m^2]	FL	Flame location [m]
b	Progress reaction variable	FAD_{max}	Maximum flame area density [m2/kg]
C_p	Specific heat [kJ/kg-K]	IFA	integrated flame area [m^2]
D	Diameter [m]	Ka	Karlovitz number [chemical time scale / time time]
D_t	Mass diffusivity [m^2/s]		

K_t Flame stretch [1/s]
K_u Thermal conductivity [W/m-K]
Ka_δ Second Karovitz number [reaction zone thickness * Ka]
h Enthalpy [kJ/kg]
ℓ Turbulent length scale [m]
ℓ_f Flame thickness [m]
M Dynamic viscosity [Nm/S^2]
Pr Laminar Prandtl number of the burnt gas [C_p μ / k_u]
P_o Reference pressure [KPa]
P_u Pressure of the unburned gas [KPa]
Sc Schmidt number [υ_t /D_t]
S_L Laminar flame speed [m/sec]
U Velocity [m/sec]
T_o Reference Temperature [K]
T_u Temperature of the unburned gas [K]
TKE Turbulent kinetic energy [kJ/kg]
u' Fluctuation velocity [m/sec]
u'' Fluctuation velocity with respect to the Favre-averaging [m/sec]
v Volume [m^3]
x_k Coordinate component [m]
Y Axial direction along the diffuser [m]
Y_{ft} Mass fraction of unburnt gas [%]
Y_f Mass fraction [%]
Y_{res} Residual of fuel mass fraction [%]
W Constant of laminar flame speed
Z Constant of laminar flame speed

GREEK SYMBOLS

δ_l The thermal boundary layer [m]
ε Turbulent dissipation rate [m^2/s^3]
η Constant of laminar flame speed [-]
Λ Constant of laminar flame speed [-]
λ Air – fuel ratio actual to stoichiometric [-]
μ_b Molecular viscosity the burnt gas
υ_t Kinematic viscosity [m/s]
ξ Constant of laminar flame speed [-]
ρ Density [kg/ m^3]
ρ_u Density of the unburned [kg/m^3]
Σ Flame area density per volume [m^2 /m^3]
σ Flame area density per mass [m^2 /kg]
ϕ Equivalence ratio of the fuel [-]
ψ Constant of laminar flame speed [-]

ABBERVIATIONS

$\tilde{c}$ Un-normalized reaction variable
B Model parameter
CFM Coherent flame model
S Source term
S_f Source term in terms of fuel mass fraction
S_Σ Source term in terms of flame area density
TI Turbulence intensity
α Constant parameter of the CFM model
β Constant parameter of the CFM model
Γ_k The ratio of the flame stretch to the k – epsilon
Γ_p The flame production due to the stretch
Γ_q The flame quench due to the stretch
$\widetilde{\ldots}$ The Favre property
$\overline{\ldots}$ The averaged property
$\ldots''$ The Favre property with fluctuation

INTRODUCTION

A large portion of the energy used for household heating and electricity production is generated from the combustion of fossil fuel. Combustion processes play a significant role in the design of combustion devices, such as gas turbines in power plants and spark ignition engines in transportation vehicles. The understanding of the combustion–turbulence interaction is crucial to improvement of the combustion systems. Most of the studies associated with the combustion–turbulence interaction focused on the impact of turbulence on flames.

Many researchers, such as (Marble and Broadwell, 1977; Borghi, 1989; Duclos et al., 1993; Zimont et al., 1998; Echekki and Mastorakos, 2011; and Veynante and Vervisch, 2002), have proposed models to investigate the impact of turbulence on combustion and understand the physical burning process. Most studies have modeled the source terms of species equations. The coherent flame model is one of these models. This model contributes significantly to the effect of turbulence on combustion and is fundamentally based on flamelet concepts. The coherent flame model was proposed by (Marble and Broadwell, 1977), who solved the source term in the species transport equation by adopting the fuel mass fraction and flame area density. Wrinkling on the flame front, which is caused by turbulence (subject to the motions of eddies), leads to an increase in the area of the flame front. This increase in area is described by the flame surface area per unit volume, which is called the flame area density. Therefore, flame area density is a central quantity in the premixed turbulent combustion model, especially when one of the objectives is to understand the effect of turbulence on combustion.

In most flame models, the effect of turbulence is included in turbulence intensity and turbulence length scales. Therefore, many researchers have investigated the effect of turbulence length scales and turbulence intensity on the turbulence–combustion interaction. Clavin and Joulin (1983) studied premixed flames in a large-scale, high-intensity turbulent flow and observed that the flame stretch may control the flame shape and motion of the front. Furthermore, the stretch is divided into two parts, namely, strain tensor rates and mean curvature. Tang and Chan (2006) examined the impact of turbulence on flame area density and flame brush thickness in a rod-stabilized V-shaped flame. They compared flame area density by using two different models and indicated that the discrepancy between the two models becomes increasingly obvious when turbulence intensity is increased.

Gülder and Smallwood (2007) analyzed the effect of medium and high turbulence intensities on the flame area

density of a turbulent premixed flame in a Bunsen burner. They achieved the largest value of flame area density at the highest turbulence intensity. Furthermore, they observed that turbulence intensity does not significantly influence the integrated flame surface density across the flame brush. Hartung et al. (2008) experimentally examined the influence of heat release on the turbulence and scalar–turbulence interaction in premixed combustion. They indicated that heat release influences the size, shape, and characteristics of the recirculation region behind the bluff body. The heat releases are associated with an increase in the length and time scales of the turbulence.

Han and Huh (2008) investigated the role of displacement speed in the evolution of flame surface density with different Lewis numbers and turbulence intensities. They observed a high turbulent burning velocity at a high turbulence intensity. They concluded that a high turbulent flame speed results from an increase in the total mean consumption speed. They also observed the flame surface density inluenced by the propagation flame and tangential strain. They found that the mean strain changes linearly with turbulence intensity. Fru et al. (2011) investigated a premixed flame with various equivalence ratios under high turbulence intensities by performing a direct numerical simulation. They determined that the consumption speed initially increases linearly. A bending zone then occurs before the consumption speed decreases (quenching limit) with the increase in turbulence intensity. The increase in turbulence intensity leads to an increase in the fuel consumption rate. Bagdanavicius et al. (2015) investigated the influence of stretch rate on flame surface densities in a turbulent premixed flame with a temperature and pressure of up to 673 K and 1.25 MPa, respectively. They derived a new overall correlation for the probability of the burning factor in terms of strain rate and Markstein number at different Karlovitz numbers. They observed that the area that is related to turbulent burning velocity normalizes the wrinkling on the flame surface.

The findings of previous investigations of flame front characteristics, particularly flame structure, flame shape, and flame–flow interaction, revealed a strong relationship between flame and turbulence. Despite the numerous studies that examined the effect of turbulence on flames, the flame front location has not been investigated extensively. Therefore, the influence of turbulence on flame location should be considered in an extensive investigation of a simple combustor, in which the sole effect of turbulence on the flame can be tested. In this paper, a diffuser-type combustor is selected to study the effect of the turbulence intensity and length scale on the flame location behavior without changing the mixture velocity (i.e., thermal power and combustor geometry). The diffuser shape is chosen due to the fact the flow slows down along the flow direction; consequently, the flame is predicated to propagate toward the inlet of the combustor when the flame velocity increases.

Investigation of the effect of turbulence on flame location depends on the proper selection of the flame model and geometry of the combustor. Coherent flame and *k–ε* models are used because this study is associated with the effect of turbulence on flames, which is discussed in the modeling of the flame and combustion section. In the result section, the effect of turbulence on flame location is discussed and the the behavior of turbulent kinetic energy is analyzed across different turbulence intensities and length scales.

MODELING OF FLAME AND COMBUSTION

For reacting flows, the transport equations of chemical species and energy are used to describe the main reactive and thermal processes. In this study, the *k–ε* model is selected to deal with turbulent flow. The *k–ε* model can calculate turbulent length scales and turbulence intensities by using the turbulent kinetic energy and turbulence dissipation rate. All these formulations and equations are solved with the Reynolds-averaged Navier–Stokes (RANS) method, which is among the numerical techniques available for the simulation of turbulent premixed combustion (Tangermann et al., 2010). Furthermore, Favre averaging is used to solve the equations involved in this model because of the variation in density that occurs during combustion.

Therefore, the governing equations of continuity, momentum, energy, and species are formulated in terms of the Favre-averaging density of (Bray and Moss, 1977) as follows:

Continuity equation

$$\frac{\partial \bar{\rho}}{\partial t} + \frac{\partial (\bar{\rho}\,\tilde{u}_i)}{\partial x_i} = 0 \tag{1}$$

Momentum equation

$$\frac{\partial}{\partial t}(\bar{\rho}\tilde{u}_i) + \frac{\partial}{\partial x_j}\left(\bar{\rho}\tilde{u}_i\tilde{u}_j\right) = -\frac{\partial \bar{P}}{\partial x_i} + \frac{\partial}{\partial x_j}\left(\tilde{\tau}_{ij} + \bar{\tau}_{tij}\right) \tag{2}$$

Energy equation

$$\frac{\partial}{\partial t}\left(\bar{\rho}\tilde{h}\right) + \frac{\partial}{\partial x_k}\left(\bar{\rho}\tilde{u}_k\tilde{h}\right) = -\frac{\partial \bar{\rho}\,\widetilde{u_k'' h''}}{\partial x_k} - \frac{\partial}{\partial x_k}\overline{\left(\rho D_t \frac{\partial h}{\partial x_k}\right)} \tag{3}$$

In the coherent flame model, the fuel mass fraction and flame area density are solved with the source term of the species equation (Marble and Broadwell, 1977; Pope, 1988; Cant et al., 1990; CD-adapco, 2016). The transport equation of species is thus formulated in terms of the un-normalized reaction progress as follows (Meneveau and Poinsot, 1991):

$$\frac{\partial}{\partial t}(\bar{\rho}\tilde{c}) + \frac{\partial}{\partial x_k}(\bar{\rho}\tilde{u}_k\tilde{c}) = \frac{\partial}{\partial x_k}\left(\bar{\rho}\frac{\nu_t}{S_C}\frac{\partial \tilde{c}}{\partial x_k}\right) + \bar{S_f} \quad (4)$$

Where $\tilde{c}$ is un-normalized reaction progress and is defined as

$$C = Y_{ft} + Y_{res} - Y_f \quad (5)$$

The fuel mass fraction is calculated in terms of the progress reaction variable (b), which is equal to the zero for unburned gases and unity for burned gases.

$$b = \frac{c - Y_{res}}{Y_{ft} - Y_{res}} \quad (6)$$

The second term on the right side of Eq. (4) is the source term in terms of the fuel mass fraction (S_f).

$$S_f = -(\rho_u S_L \sum)(Y_{ft} - Y_{res}) \quad (7)$$

The laminar flame speed is calculated based on correlation of (Gülder, O., 1990) as follows

$$S_L = Z\,W\,\phi^{\eta}\,exp[-\xi(\phi - 1.075)^2]\left(\frac{T_u}{T_o}\right)^{\psi}\left(\frac{P_u}{P_o}\right)^{\Lambda} \quad (8)$$

where *Z = 1, W =0.446, η = 0.12, ξ = 4.95, ψ = 1.77 and Λ = - 0.2.*

In the coherent flame model, flame area density (σ) is defined as the flame area per unit mass. According to (Meneveau and Poinsot, 1991 and Boudier et al., 1992), the transport equation of species in terms of the flame area density is as follows:

$$\frac{\partial}{\partial t}(\bar{\rho}\tilde{\sigma}) + \frac{\partial}{\partial x_k}(\bar{\rho}\tilde{u}_k\tilde{\sigma}) = \frac{\partial}{\partial x_k}\left(\bar{\rho}\frac{\nu_t}{S_C}\frac{\partial \tilde{\sigma}}{\partial \tilde{x}_k}\right) + \bar{S_\Sigma} \quad (9)$$

where the source term is represented in terms of flame area density per unit volume $\sum$ and equal to

$$S_\Sigma = \alpha K_t\,\Sigma - \beta\frac{\rho_u Y_{ft} S_L\left(1 + a\sqrt{k}/S_L\right)}{\rho\, Y_f}\Sigma^2 \quad (10)$$

With regard to flame area density, the turbulence effect is represented in terms of the flame stretch, which is a function of the *k–ε* model (in other words, turbulence length scale and turbulence intensity) (Meneveau and Poinsot, 1991). Therefore, flame stretch K_t in Eq. (10) is calculated as

$$\Gamma_K = \frac{K_t}{\varepsilon/_k} = f\left(\frac{u'}{S_L}, \frac{\ell}{\ell_f}\right) \quad (11)$$

Meanwhile, Γ_K is defined as

$$\Gamma_K = \Gamma_p - B\,\Gamma_q \quad (12)$$

where Γ_p and Γ_q are the flame production and quench due to the stretch, respectively (Meneveau and Poinsot 1991). The fluctuation velocity (u') is calculated with the *k–ε* model as

$$u' = \sqrt{\frac{2}{3}\,k} \quad (13)$$

Turbulence length scale (ℓ) is also calculated with the *k–ε* model by employing turbulent kinetic energy (TKE) and turbulence dissipation rate (Pope, 2000).

$$\ell = \frac{k^{3/2}}{\varepsilon} \quad (14)$$

SETTINGS OF THE NUMERICAL SIMULATION AND TEST CASES

Propane–air mixtures are premixed upstream of the diffuser combustor with $\lambda = 1.7$, and the mass percentages of the gas components of fuel are 3.81% C_3H_8, 23.55% O_2, and 72.63% N_2. The fresh mixtures are injected at a speed of 0.3 m/s and a temperature of 300 K into the diffuser burner with an inner diameter of 10 cm and an outlet diameter of 20 cm. The length of the diffuser is 95.3 cm, the downstream diffuser outlet is constant with length 40 cm, and the angle of the half expansion of the diffuser is 3° (Figure 1).

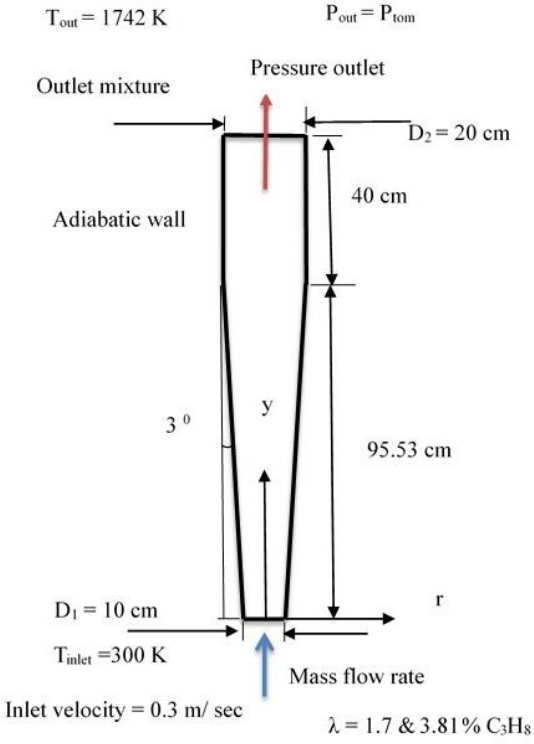

Figure 1. The geometry of the diffuser combustor and boundary conditions.

All numerical simulations are performed with the commercial STAR CCM+ version 11.02.009-R8. The simulations are conducted using the steady, 3D, coherent

flame model and one-step global reaction, which can be written as

$$C_3H_8 + 5O_2 \longrightarrow 4H_2O + 3CO_2 \qquad (15)$$

The boundary conditions imposed on the simulation model are ambient pressure and a temperature of 300 K at the inlet. The wall condition is assumed adiabatic. The output temperature was set to the temperature of the fully burned gas which 1742 K.

The conditions considered include the turbulence intensities at the inlet of the combustor from the low level (TI = 5%) to the high level (TI = 35%). Meanwhile, the turbulence length scales are set as ℓ = 1 cm to 10 cm, as shown in Table 1. The outcomes are depicted by the flame location.

Table 1. Test cases of the simulation under different TI and ℓ values at the inlet of the diffuser.

Test cases	1	2	3
ℓ	1 cm	5 cm	10 cm
TI	5 %	5 %	5 %
TI	10 %	10 %	10 %
TI	15 %	15 %	15 %
TI	20 %	20 %	20 %
TI	25 %	25 %	25 %
TI	30 %	30 %	30 %
TI	35 %	35 %	35 %

Selection number and type of mesh are necessary to ensure the accuracy of the solution. Mesh size and percent open area are selected based on the diameters and lengths of the diffuser. Polyhedral meshes are selected to build the core mesh of diffuser geometry because it provides a balanced solution for mesh generation problems. In addition, polyhedral meshes are more efficient and easier to use than tetrahedral meshes. The prism layer mesh is also utilized to deal with the core volume mesh for generating orthogonal prismatic cells next to boundaries or wall surfaces. This prism layer is crucial to enhance the accuracy of the solution. The number of mesh cells is 506,387.

Mesh independence is performed with large ranges of mesh size to assess the accuracy of the obtained results of the simulation cases. Figure 2 shows the flame location via the number of cells of the mesh for 5% turbulence intensity and 1 cm turbulence length scale. For the low number of mesh cells, a small deviation of 2 mm is detected in the flame location of the other cases. Then, the flame location is fixed with an increase in the number of mesh cells.

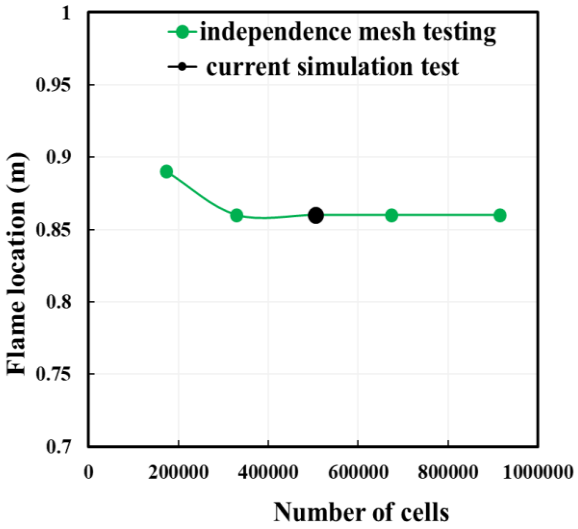

Figure 2. Flame location with the number of mesh cells for TI = 5% and ℓ = 1 cm.

RESULTS AND DISCUSSION

Understanding how the flame responds and manifests within the regime of the turbulent premixed flame is essential in analyzing the combustion–turbulence interaction at different turbulence intensities and turbulence length scales. This regime (Borghi 1989; Peters 1989; Abdel-Gayed et al., 1989) is based on velocity and turbulence scale ratios and divided into many zones depending on the dimensionless numbers, as shown in Figure 3. Changing the level of turbulence leads to a change in the location within the regimes of the premixed turbulent combustion, which leads to different physical processes. Figure 3 indicates the locations of the flame for all of the test cases. The locations of the flame are within the wrinkled and corrugated flamelet regimes.

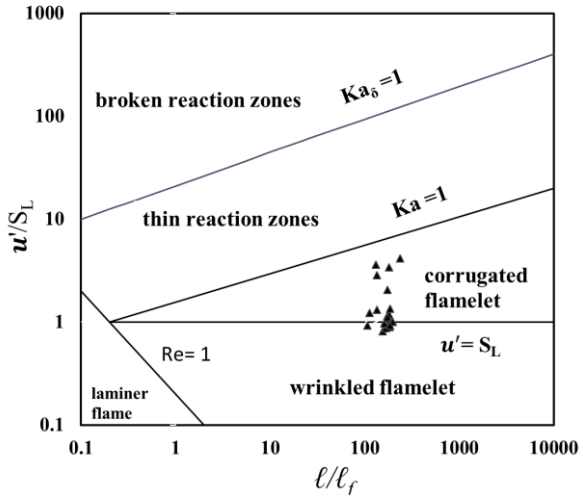

Figure 3. Locations of the flames in the turbulent combustion regime.

Temperature and flame area density are the main parameters used to determine the location of the flame front. Flame area density and temperature are represented as a function of turbulence intensity and turbulence length

scale. A line probe, which is set along the axial centerline of the diffuser, is used to obtain the main properties, such as temperature, TKE, and flame area density.

Figure 4 presents a comparison of temperature contours at various turbulence intensities and turbulence length scales. Figure 5 illustrates flame location as a function of turbulence intensity and turbulence length scale. Flame location is extracted from a stationary temperature field of 1,400 K for all cases. Figures 4 and 5 show that the flame front location generally moves toward the inlet of the diffuser with the increase in turbulence intensity for 5 and 10 cm turbulence length scales. However, this behavior depends on the values of turbulence intensities. First, the flame location moves toward the inlet of the diffuser combustor with an increase in turbulence intensity from 5% to 10%. Second, the flame stabilizes at turbulence intensities of 10% and 15% before decreasing with an increase in turbulence intensity to 20%, 25%, 30%, and 35%.

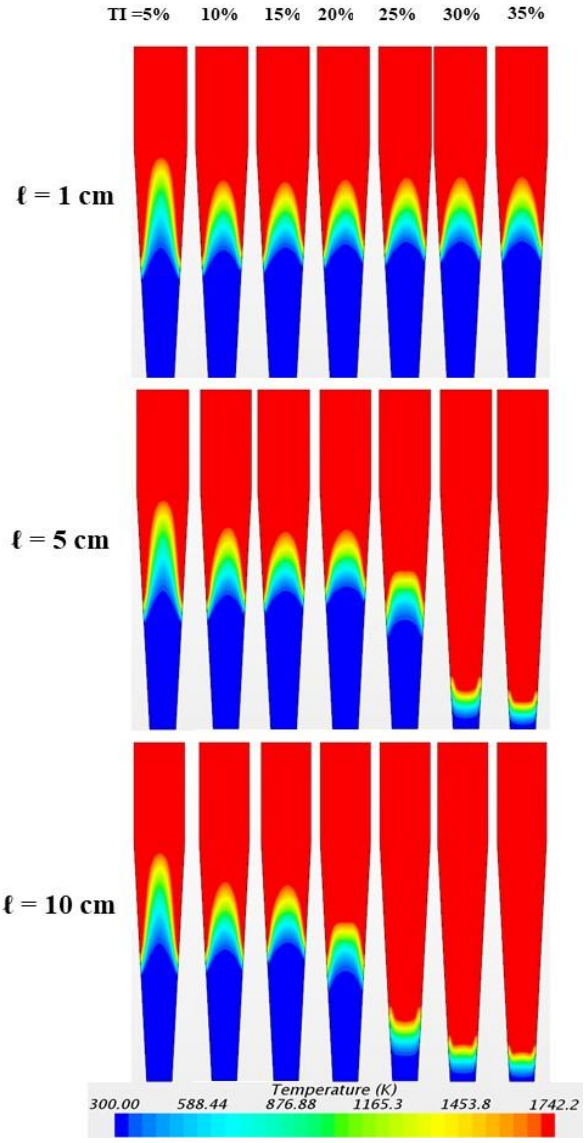

Figure 4. Temperature contours with various turbulence intensities and turbulence length scales at the inlet of the diffuser.

The behavior of the flame location for the 1 cm turbulence length scale is also observed. First, the flame location moves toward the inlet of the diffuser combustor with an increase in turbulence intensities from 5% to 10%. Second, the flame location stabilizes with a further increase in the turbulence intensity, as illustrated in Figure 5.

The effect of turbulence intensity on the movements of the flame location at the inlet is more visible with the 5 and 10 cm turbulence length scales (high turbulence Reynolds number) and 30% and 35% turbulence intensities compared with a low turbulence intensity and small turbulence length scale. The results generally show that the flame location is dependent on turbulence intensity and turbulence length scale.

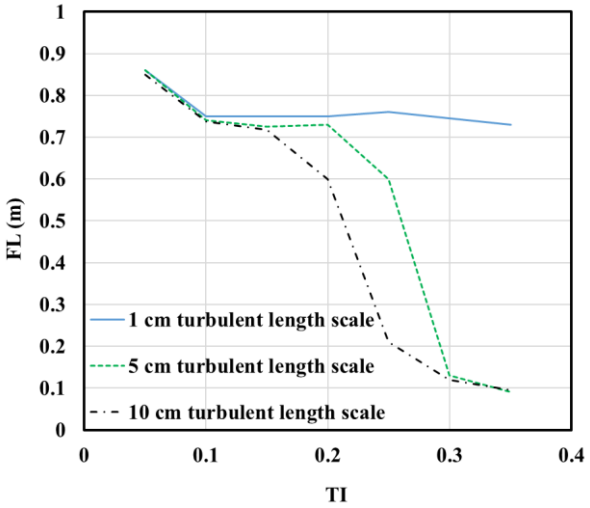

Figure 5. Flame location on the axial centerline of the diffuser combustor with various turbulence intensities and turbulence length scales.

Comparative impacts of turbulence on flames front have been shown by many studies. For instance, Yuan et al. (2006) analyzed the effects of turbulence intensity on the flame by varying turbulence intensities within ranges of 1% to 50%. They observed that hydrodynamic instability dominates the development of flame at low level of turbulence intensities of 1% to 5%. Meanwhile, turbulence dominates the process and wrinkles the flame front at high turbulence levels of 50%. Along these lines, it was set the range of turbulence intensities within 5% to 35%, and the outcomes show the expected impact of turbulence on the flame, that is, the turbulent flame velocity increases with an increase in turbulence intensity and moves to the inlet of combustor.

In addition to the change in the flame location, the flame shape changes with an increase in turbulence intensity (greater than 25%) and turbulence length scales (5 and 10 cm). The flame shape can be convex or concave. Many types of flame shapes exist depending on the shape factor, which is based on the flame position and axis planes (Chakraborty and Cant, 2006; and Kerl et al., 2013).

Three types of the flame shapes introduced by Kerl et al. (2013) in a diffuser burner at an annular swirling flow that included parabolic, elliptic, and hyperbolic. Given

that their work is the most similar to the present work, the flame shapes obtained in the present work can be considered realistic.

The behavior of TKE is crucial in revealing the characteristics of turbulence–combustion interactions. Therefore, TKE is plotted together with turbulence intensities and turbulenent length scales in the same graph. A physical explanation for flame location behavior with the change in turbulence intensity and turbulence length scale due to the variation in TKE with changing TI and ℓ is also provided.

Turbulence intensity and turbulence length scale are functions of TKE, as illustrated in Equations. (11) and (12). Therefore, considering TKE is essential in understanding the effect of turbulence on flame location. The TKE along the axial centerline of the diffuser combustor is measured using a line probe.

Figures 6a, 6b, and 6c show the variation in the TKE along the centerline of the diffuser combustor with turbulence intensity and turbulence length scales of 1, 5, and 10 cm, respectively. TKE initially decays and then increases in the flame region and further downstream. The increase in TKE occurs within the region of combustion, starting with a flame temperature of T = 1,400 K. At a constant turbulence length scale (Equation (14)), increasing the turbulence intensity means an increase in the turbulence dissipation rate (ε). In addition, the decay rate of TKE downstream of the inlet is larger than that at a high turbulence intensity.

Figure 6a also shows that the TKE for 5% turbulence intensity is less than that for 10% turbulence intensity. The development of all the other TKE cases is similar for other values of turbulence intensities. This behavior is similar to that of the flame shown in Figure 5. The flame moves toward the inlet of the diffuser with an increase in the turbulence intensity from 5% to 10%. Subsequently, the flame location stabilizes with an increase in the turbulence intensity.

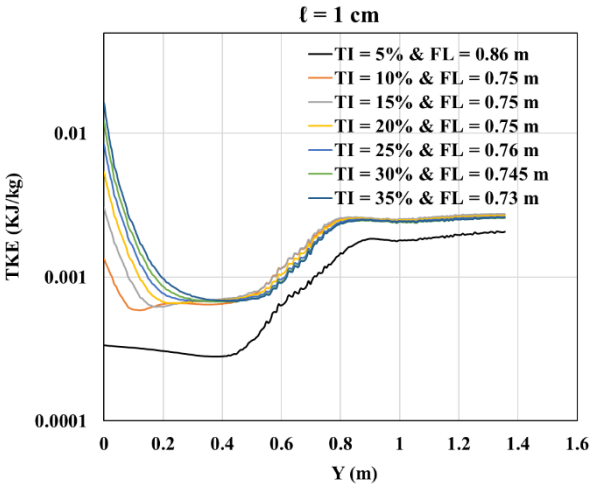

Figure 6a. TKE along the axial centerline of the diffuser combustor at various turbulence intensities and at 1 cm turbulence length scale.

Figure 6b shows TKE with turbulence intensity for the 5 cm turbulence length scale. Two sharp TKE peaks are observed with the increase in turbulence intensity to 30% and 35%. No significant differences are observed at turbulence intensities of 10% and 15% in the flame regions. Hence, the flame location for a low turbulence intensity is stabilized, and the flame location sharply moves to the inlet of the diffuser combustor at turbulence intensities of 30% and 35%, as illustrated in Figure 5.

Figure 6b shows that the curve of TKE for turbulence intensity = 0.25 is less than the curve of TKE for turbulence intensity = 0.1, 0.15, and 0.2 after y = 0.8 m. In addition, the curve of turbulence intensity = 0.35 is less than the curve of turbulence intensity = 0.3 after y = 0.8 m. This behavior is related to the drop in the flame location and the deceleration of the flow in the diffuser. More specifically, when the flame pulled towards the inlet the flow with increased TKE at the wake the of the flame is exposed to the deceleration of the mean flow. The deceleration of the mean flow augments the decay of the TKE. Therefore, depending on the flame location in the diffuser, cases with higher TKE at the inlet might have lower TKE at far downstream locations.

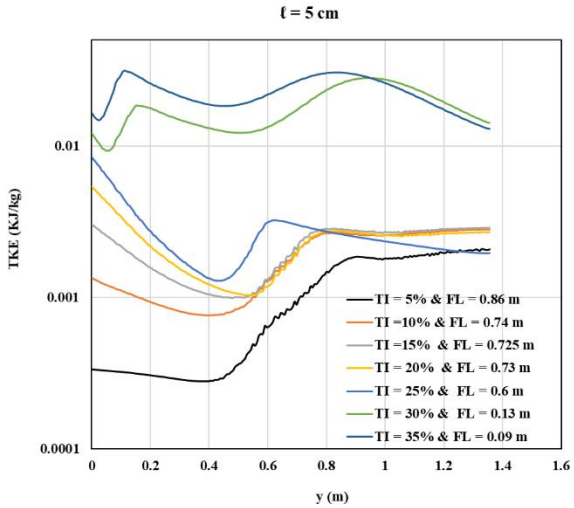

Figure 6b. TKE in the axial centerline of the diffuser at various turbulence intensities and at 5 cm turbulence length scale.

Figure 6c shows the TKE for various turbulence intensities and for the turbulence length scale of 10 cm. Three sharp TKE peaks are observed with the increase in turbulence intensity to 25%, 30% and 35%. No significant differences are observed at turbulence intensities of 10%, 15%, and 20% in the flame regions. Hence, the flame location for a low turbulence intensity is stabilized, and the flame location sharply moves to the inlet of the diffuser combustor at turbulence intensities of 25%, 30% and 35%, as illustrated in Figure 5.

Figure 6c shows that the curve of TKE at turbulence intensity = 0.2 is less than the curve of TKE at turbulence intensity = 0.1 and 0.15 after y = 0.8 m. In addition, the curve of turbulence intensity = 0.3 is less than the curve of turbulence intensity = 0.25 after y = 0.9 m. This behavior is related to the drop in the flame location and the deceleration of the flow in the diffuser. More

specifically, when the flame pulled towards the inlet the flow with increased TKE at the wake the of the flame is exposed to the deceleration of the mean flow. The deceleration of the mean flow augments the decay of the TKE. Therefore, depending on the flame location in the diffuser, cases with higher TKE at the inlet might have lower TKE at far downstream locations.

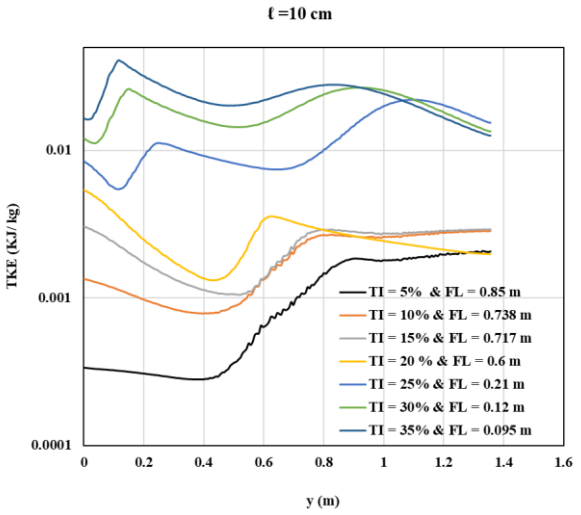

Figure 6c. Variation in TKE along the axial centerline of the diffuser combustor at various turbulence intensities for the 10 cm turbulence length scale.

However, important observations can be formulated for TKE with varying turbulence intensities and turbulence length scales. The flame location moves toward the inlet of the combustor with a concurrent increase in turbulence intensity and TKE. In addition, the highest value of TKE is observed at the lowest value of the flame location. This behavior is due to the increase in TKE, which increases the value of $S_{\sum}$ in Equation (10). Thus, the combustion zone becomes narrow, and the flame is pushed toward the inlet of the combustor.

Flame area density is also used to indicate the flame response in this study. Figures 7 and 8 show the maximum and integrated flame area (IFA) density with respect to turbulence intensities and turbulence length scales, respectively. The maximum flame area density remains constant with the increase in turbulence intensity for a low turbulence length scale (ℓ = 1 cm) (Figure 7). Meanwhile, for ℓ = 5 and 10 cm, the maximum flame area density remains constant with the increase in turbulence intensity until it reaches 20% and then increases with the increase in turbulence intensity to 25% and 30% before becoming constant again.

Gülder and Smallwood (2007), who examined the flame area density in a premixed turbulent flame at various levels of turbulence intensity in a Bunsen burner and concluded that the maximum flame surface density vary with turbulence intensity but show no systematic correlation with it, as it is the case in the present investigations. Integrated flame area has almost the same values, as illustrated in Figure 8.

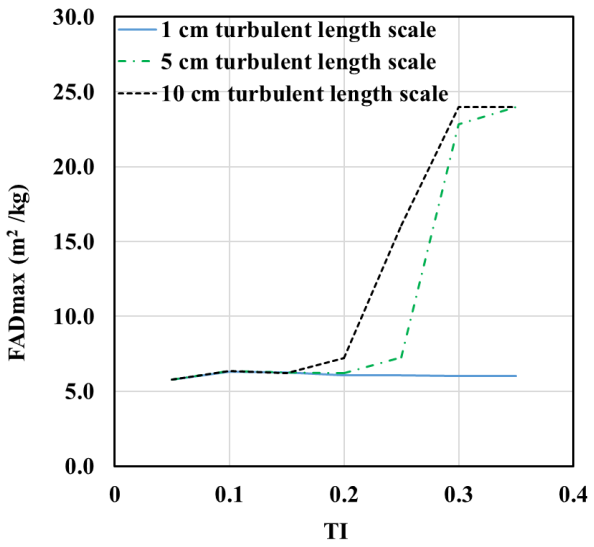

Figure 7. Maximum flame area density FAD_{max} along the axial centerline of the diffuser with various turbulence intensities and length scales values.

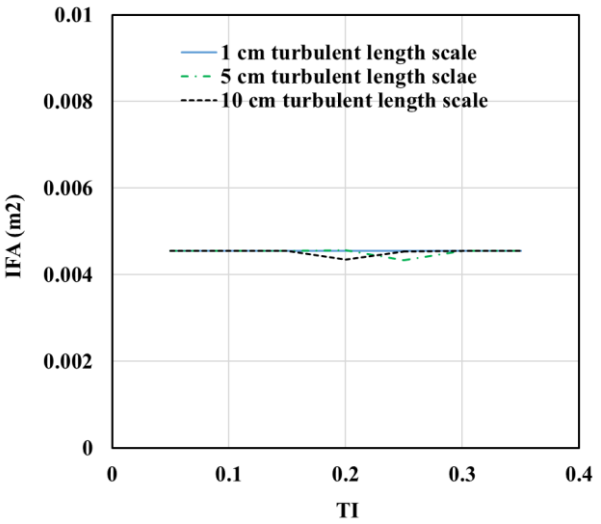

Figure 8. Integrated flame area over the diffuser for various turbulence intensities and length scales values.

CONCLUSIONS

The effects of turbulence intensity and turbulence length scale on flame location are investigated numerically using a diffuser combustor. The results indicate that turbulence intensities and turbulence length scales exert a significant effect on the flame location of premixed combustion. The behavior of the flame location depends on the behavior of TKE, which changes with a change in turbulence intensity and turbulence length scale.

Generally, the flame front moves toward the inlet of the combustor with the increase in turbulence intensity. For the moderate and high turbulence length scales, the flame location initially decreases with the increase in turbulence intensity, and the flame location then stabilizes before decreasing with an increase in turbulence intensities.

However, the behavior is different for the low turbulence length scale. The flame location reduces with the increase in turbulence intensity from low turbulence intensities. Then, the flame location stabilizes with the increase in turbulence intensity. This behavior depends on TKE. In addition, with the change in the flame location, the flame shape changes with the increase in turbulence intensity to a high level and with the 5 and 10 cm turbulence length scales.

We conclude that turbulence intensity and turbulence length scale simultaneously influence the flame location, flame shape, and flame area density.

ACKNOWLEDGMENT

This work is supported by Ozyegin University in Istanbul, Turkey, and Tikrit University in Tikrit, Iraq. The authors would like to thank the Scientific and Technological Research Council of Turkey (TÜBİTAK) for providing financial support for this research through the 114C113 Project.

REFERENCES

Abdel-Gayed R. G., Bradley D., and Lung F. K.-K., 1989, Combustion Regimes and the Straining of Turbulent Premixed Flames, *Combustion and Flame*, 76, 213–218.

Bagdanavicius A., Bowenb P. J., Bradleyc D., Lawes M. and Mansour M. S., 2015, Stretch Rate Effects and Flame Surface Densities in Premixed Turbulent Combustion up to 1.25 MPa, *Combustion and Flame*, 162, 4158-4166.

Borghi R., 1989, Turbulent Combustion Modelling, *Progress in Energy and combustion*, 14, 145-295.

Boudier P., Henriot S., Poinsot T. and Baritaud T., A, 1992, Model for Turbulent Flame Ignition and Propagation in Spark Ignition Engines, *Proceedings of the Combustion Institute*, 24, 503-510.

Bray, K. N C, Moss and J. B., 1977, a Unified Statistical Model of the Premixed Turbulent Flame, *Acta Astronautica*, 4, 291-219.

Cant R. S., Pope S. B., and Bray K. N. C., 1990, Modelling of Flamelet Surface-to-Volume Ratio in Turbulent Premixed Combustion, *Twenty-Third Symposium Internationational on Combustion/The Combustion Institute*, Cornell University, New York, 809–815.

CD-adapco, 2016, *STAR CCM+ Documentation and User Guide*, Version 11.02.009-R8, Melville, USA.

Chakraborty N., and Cant R. S., 2006, Statistical Behavior and Modeling of Theflame Normal Vectorin Turbulent Premixed Flames, *Numerical Heat Transfer, Part A: Applications: An International Journal of Computation and Methodology*, 50, 623–643.

Clavin, P., and G. Joulin., 1983, Premixed Flames in Large Scale and High-Intensity Turbulent Flow, *Journal de Physique Lettres*, 44, 1–12.

Duclos J M, Veynante D., and Poinsot T., 1993, A Comparison of Flamelet Models for Premixed Turbulent Combustion, *Combustion and Flame*, 7, 101–117.

Echekki T. and Mastorakos E., 2011, *Turbulent Combustion Modeling* (First Ed.) Springer-Verlag Berlin Heidelberg, New York:.

Fru G., Thévenin D., and Janiga G., 2011, Impact of Turbulence Intensity and Equivalence Ratio on the Burning Rate of Premixed Methane-Air Flames, *Energies*, 4, 878–893.

Gülder Ö. L., 1990, Turbulence Premixed Flame Propagation Models for Different Combustion Regimes, *23rd Symposium International on Combustion, the Combustion Institute*, 23, 743-750.

Gülder, Ö. L., and Smallwood G. L., 2007, Flame Surface Densities in Premixed Combustion at Medium To High Turbulence Intensities, *Combustion Science and Technology*, 179, 191–206.

Han Insuk, and Huh K. Y., 2008, Roles of Displacement Speed on Evolution of Flame Surface Density for Different Turbulent Intensities and Lewis Numbers in Turbulent Premixed Combustion' *Combustion and Flame*, 152, 194–205.

Hartung G., Hult J., Kaminski C. F., Rogerson J. W. and Swaminathan N., 2008, Effect of Heat Release on Turbulence and Scalar-Turbulence Interaction in Premixed Combustion, *Physics of Fluids*, 20, 035110(1–16).

Kerl J., Lawn C., and Beyrau F., 2013, Three-Dimensional Flame Displacement Speed and Flame Front Curvature Measurements Using Quad-Plane PIV, *Combustion and Flame*, 160, 2757–2769.

Marble F. E. and Broadwell J. E., 1977, *Coherent Flame Model for Turbulent Chemical Reactions*, Project Squid Technical Report TRW-9-PV, Purdue Unversity, Indiana, USA.

Meneveau C., and Poinsot T., 1991, Stretching and Quenching of Flamelets in Premixed Turbulent Combustion, *Combustion and Flame*, 86, 311–32.

Peters N. 1989. 'Length and Time Scales in Turbulent Combustion, Turbulent Reactive Flows, 242–56. *In Borghi R., Murthy S.N.B., Editors, Turbulent Reactive Flows, Lecture Notes in Engineering*, 40, 242–256.

Pope S.B., 1988, The Evolution of Surface in Turbulence'. *Int. J. Engng Sci*, 26, 445–469.

Pope S. B., 2000, *Turbulent Flows* (First Ed.), Cornell University, New York, USA.

Stiesch G., 2003, *Modeling Engine Spray and Combustion Processes* (First Ed.), Springer-Verlag Berlin Heidelberg, Hannover, Germany.

Tang B. H. Y., and Chan C. K., 2006, Simulation of Flame Surface Density and Burning Rate of a Premixed Turbulent Flame Using Contour Advection' *Combustion and Flame*, 147, 49–66.

Tangermann E., Keppeler R., and Pfitzner M., 2010, 'Premixed Turbulent Combustion Models for Large Eddy and RANS Simulations, *Proceedings of ASME Turbo Expo : Power for Land, Sea and Air*, 2, 203-212.

Veynante, D. and Vervisch L., 2002, Turbulent Combustion Modeling, *Progress in Energy and Combustion Science*, 120, 193–266.

Yuan, J., Ju Y. and Law C. K., 2006, Effects of Turbulence and Flame Instability on Flame Front Evolution, *Physics of Fluids*, 8, 104105-1– 104105-9.

Zimont V. L., Polifke W., Bettelini M and Weisenstein W., 1998, An Efficient Computational Model for Premixed Turbulent Combustion at High Reynolds Numbers Based on a Turbulent Flame Speed Closure, *J. Eng. Gas Turbines & Power*, 120, 526–532.

Ibrahim Thamer Nazzal has received his bachelor and master degrees in Mechanical Engineering from Tikrit University, Iraq in 2001, 2004 respectively. He is currently a Ph.D. student at Ozyegin University and his interested research about the turbulent combustion, internal combustion engine and heat exchangers.

Dr.-Ing. Özgür Ertunç has received his bachelor and master degree in Aeronautical Engineering from METU Ankara, Turkey. Later, he joined to the Institute of Fluid Mechanics (LSTM) at FAU Erlangen-Nuremberg. He got his Dr.-Ing. degree in 2006 for his research on turbulent flows. He established there two research groups, namely Unsteady Fluid Mechanics and Fluid Dynamics and Turbulence. Since 2013 he is a faculty in the Mechanical Engineering of Özyeğin University, where he established the Fluid Dynamics and Spray Laboratory. His research is on turbulence and its technological applications, combustion, droplets and sprays.